ACS OMEGA

Open Access

http://pubs.acs.org/journal/acsodf

Article

In Silico Modeling and Characterization of Epstein−Barr Virus Latent Membrane Protein 1 Protein

Dayang-Sharyati D. A. Salam, Kavinda Kashi Juliyan Gunasinghe, Siaw San Hwang, Irine Runnie Henry Ginjom, Xavier Chee Wezen,* and Taufiq Rahman*

Cite This: *ACS Omega* 2024, 9, 49422−49431

Read Online

ACCESS | Metrics & More | Article Recommendations | Supporting Information

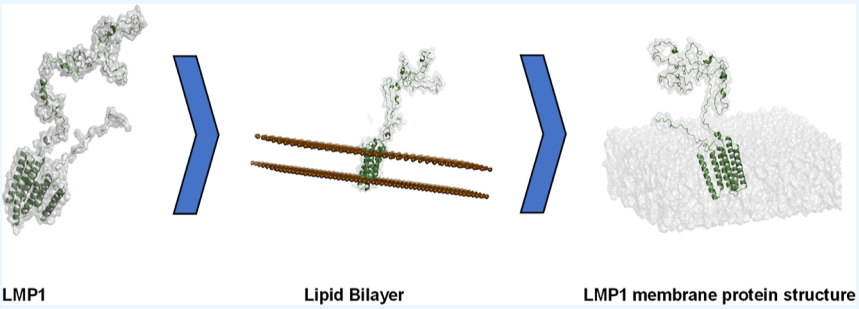

ABSTRACT: Latent membrane protein 1 (LMP1) plays a crucial role in Epstein−Barr virus (EBV)'s ability to establish latency and is involved in developing and progressing EBV-associated cancers. Additionally, EBV-infected cells affect the immune responses, making it challenging for the immune system to eliminate them. Due to the aforementioned reasons, it is crucial to understand the structural features of LMP1, which are essential for the development of novel cancer therapies that target its signaling pathways. To date, there is yet to be a complete LMP1 protein structure; therefore, in our work, we modeled the full-length LMP1 containing the short cytoplasmic N-terminus, six transmembrane domains (TMDs), and a long-simulated C-terminus. Our model showed good stability and protein compactness evaluated through accelerated-molecular dynamics, where the conformational ensemble exhibited compact folds, particularly in the TMDs. Our results suggest that specific domains or motifs, predominantly in the C-terminal domain of LMP1, show promise as potential drug targets. As a whole, our work provides insights into key structural features of LMP1 that will allow the development of novel LMP1 therapies.

1. INTRODUCTION

Epstein−Barr Virus (EBV) is a double-stranded DNA virus that is commonly contracted by humans. It is estimated that over 90% of the world's population has contracted EBV at some point in their lives.[1] Latent membrane protein 1 (LMP1) is a protein encoded by the EBV and plays a crucial role in EBV's ability to establish latency. In this state, the virus persists in infected cells without actively replicating. It is a viral oncogene that promotes cell proliferation, survival, and migration while inhibiting apoptosis.[2] LMP1 plays a critical role in developing and progressing EBV-associated cancers. EBV can cause a range of diseases that include infectious mononucleosis, Burkitt lymphoma, nasopharyngeal carcinoma, and Hodgkin lymphoma.[3] It can also alter the immune response to EBV-infected cells, making it more difficult for the immune system to eliminate. This is due to EBV latency, immune evasion, and cellular transformation. When EBV enters a latent phase, the virus is not actively replicating but its DNA remains in the cell. This makes it harder for the immune system to detect and destroy the infected cell.[4,5] EBV then encodes proteins interfering with the immune system's ability to recognize and kill infected cells. In some cases, EBV can transform a B cell into a cancerous cell. It is a multifunctional protein that can mimic the signaling of several cellular proteins, including CD40, B-cell receptor, and tumor necrosis factor receptor.[6−8] This allows LMP1 to activate various cellular signaling pathways, including NF-κB and MAPK.[9−11] Therefore, targeting LMP1 with methods such as monoclonal antibodies, small-molecule inhibitors, and gene therapy presents a promising strategy for treating EBV-related pathogenesis.

The structure of LMP1 has provided essential insights into how LMP1 mediates its oncogenic and transforming activities. LMP1 refers to the EBV latent membrane protein type I with a short cytoplasmic N-terminus (NTER), six transmembrane

Received: July 26, 2024
Revised: November 19, 2024
Accepted: November 22, 2024
Published: December 2, 2024

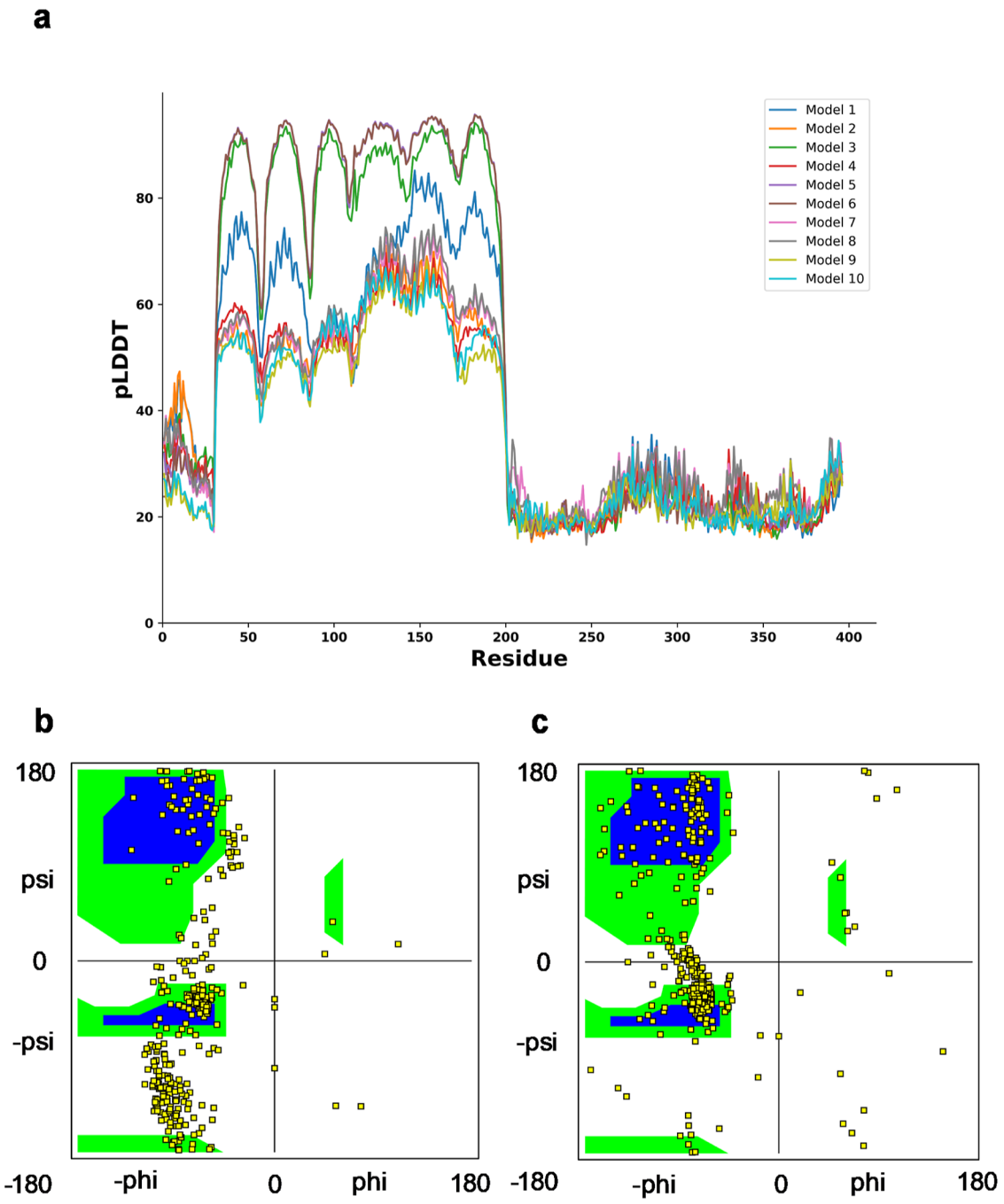

Figure 1. (a) pLDDT score per position for the 10 predicted models generated by Alphafold2. (b) Ramachandran plot for predicted protein model 3 of Alphafold2. (c) Ramachandran plot for our predicted LMP1 protein structure. The Ramachandran plot showing two core regions (blue color) and three allowed regions in the three separate boxes (green color). The beta-sheet region occupies the left-top box, the α helix at the lower-left box, and the left-handed helix at the top-right box.

domains (TMDs), and a long cytoplasmic C-terminus.[12] The TMD of LMP1 is characterized by a noncanonical fold that supports symmetric dimerization and higher-order oligomerization. TMD anchors the protein to the cell membrane, allowing it to interact with other membrane-associated proteins.[13] The NTER domain is short (24 amino acids) and located on the cytoplasmic side of the membrane and contains binding sites for various cellular proteins. Meanwhile, the C-terminus contains cytoplasmic activation regions (CTARs), which mediate the oncogenic and transforming activities of LMP1.[14] The domain is large (200 amino acids) and located on the cytoplasmic side of the membrane, containing several functional motifs involved in signal transduction.

The cytoplasmic NTER and CTAR of LMP1 contain disordered regions important for LMP1's ability to interact with multiple cellular proteins and activate various signaling pathways.[15] These regions lack a fixed, stable structure and may become more structured upon interaction with other molecules. The extent of intrinsic disorder varies across different LMP1 domains and can differ depending on the prediction method used. A study suggested that LMP1 is an intrinsically disordered protein, and our previous study also

https://doi.org/10.1021/acsomega.4c06868
ACS Omega 2024, 9, 49422−49431

showed that up to 40% of the LMP1 protein might be intrinsically disordered.[16,17] To date, no crystal structure of LMP1 is available; as such, we attempted to model the structure of LMP1 to guide future drug design against LMP1 using in silico methods.

In silico methods, such as protein prediction using AlphaFold2, have become a key aspect in understanding protein structure and dynamics. AlphaFold2 is a protein structure prediction tool developed by DeepMind.[18] It uses a deep learning method to predict the 3D structure of a protein from its amino acid sequence. This breakthrough technology has several critical applications. First, it aids in understanding protein function at a molecular level, which is crucial in various biological studies.[19] Additionally, AlphaFold2 expedites the drug discovery process by providing valuable insights into the structure of proteins targeted by drugs.[20] Lastly, it gives the ability to predict protein structures accurately.[21]

Additionally, molecular dynamics (MD) simulations are a valuable computational technique for studying protein behavior at the atomic level. This method uses classical mechanics to simulate protein dynamics by treating atoms as tiny balls and calculating their interactions based on their positions and forces. MD simulations require powerful computers or specialized hardware due to their computational complexity. They provide insights into protein folding, ligand binding, protein−protein interactions, and protein stability.[22] While AlphaFold2 predicts protein structures, MD simulations reveal how these structures change and function. In our work, we used AlphaFold2 and MD simulations to understand the protein dynamics of LMP1. This paper is the first to present the complete predicted structure of the LMP1 protein MD simulation.

2. RESULTS AND DISCUSSION

2.1. Evaluation of the LMP1 Protein Structure. First, we used protein structure prediction tools namely AlphaFold2 and GalaxyWeb to refine our LMP1 protein model that we constructed previously.[16] We selected the top model based on the models that showed high predicted local distance difference test (pLDDT) values on the AlphaFold2 and GalaxyWeb. Based on our model, we observed that the residues between 35 and 200 showed high accuracy, whereas some models (model 3 and model 6) showed a pLDDT value exceeding 90 (Figure 1). These residue ranges are in the TMD of LMP1. A study by Veit et al. produced similar results when they predicted the structure of porcine respiratory and reproductive syndrome virus dimer using AlphaFold2.[23] However, the N-terminal domain (residue from number 0 to 35) and the CTAR (residue of more than 200) have values lower than 50, suggesting that the prediction on these ambiguous regions is not experimentally conclusive since there is not much structural data available.

We also used the confidence score of the prediction (between 0 and 1) to assess the LMP-1 model quality. The confidence scores indicate how confident AlphaFold2 is in its prediction involving different aspects of protein structure and function, particularly inferred post-translational modifications (IPTMs) and post-translational modifications (PTMs). IPTMs are modifications to a protein that occur after it has been synthesized. In the context of AlphaFold2 or any protein structure prediction tool, IPTM would refer to the predicted or IPTMs based on the protein's sequence and other factors. Meanwhile, PTMs are actual modifications that occur to proteins after they are translated from mRNA. PTMs regulate protein function, stability, localization, and interactions with other molecules. They can significantly impact a protein's structure and activity. AlphaFold2 specifically predicts the 3D structure of proteins based on their amino acid sequences, considering evolutionary information and other data. While AlphaFold2 can predict the 3D structure of proteins with high accuracy, it does not explicitly predict PTMs. All the 10 model multimers predicted by AlphaFold2 ranged from 0.108 to 0.152, suggesting that the predicted model is naturally disordered or lacks sufficient information. Based on the ranking, model 3 has the best score with 0.152 confidence. The graph suggests that the high PLDDT coupled indicate the better-predicted model performance of LMP1 model 3, similar to our LMP1 predicted structure (Figure 1a). A Ramachandran plot was also plotted to showcase both resemblances through the Phi (Φ) and Psi (Ψ) angles, which define a protein's backbone geometry. Our LMP1 model showed that most of the residues fall between the core regions of the beta-sheet, α helix, and left-handed helix regions, representing the most energetically favored conformations (Figure 1b,c). These conformations consisted mainly of the left-handed α helix and beta-sheet structures, as exhibited in the TMD of LMP1.

Previous studies on LMP1 suggested that the dimeric form of protein structure is associated with its raft localization and activation and that it is active only in its oligomeric form, specifically the dimeric and trimeric forms.[24,25] The oligomeric form of LMP1 is critical for its function and activation, and its structure and interactions are essential for the LMP1 role in various cellular processes. Therefore, we also investigated the LMP1 protein structure using a program available on GalaxyWeb called GalaxyHomomer. Software is used to predict the structure of proteins composed of identical subunits known as homo-oligomers. These proteins are generated when individual protein chains, monomers, come together. GalaxyHomomer includes extra processes to improve the accuracy of the projected structure. This includes modeling the protein's flexible sections and revising its overall structure. The ab initio docking results of GalaxyHomomer suggested that our LMP1 protein structure consisted of dimeric and trimeric structure conformation such as homo-oligomer (Supporting Information Table S1). With the highest docking score value of 2350.543 and interface area of 2279.7 (in Å^2), the predicted model 1 structure consisting of dimer units was similar to the model indicated through AlphaFold2 (Supporting Information Figure S1). After the validation of our predicted LMP1 protein structure, we embedded the LMP1 protein in the membrane, as described in Section 4. There are various examples of validation in computational biomechanics, emphasizing the importance of experimental data in validating models. We validated our models with the intention of applying predictions to further analysis and experimentation, particularly in the context of patient outcomes. However, comparing model predictions with experimental results to establish credibility in computational modeling is also important.

2.2. Simulating LMP1 Using Accelerated MD Simulation. After evaluating the predicted LMP1 protein structure, we simulated the protein using accelerated MD (aMD) simulation for 500 ns in triplicates. The aMD is designed to accelerate the sampling of the phase space by reducing energy barriers, making it more efficient for studying complex systems such as protein folding. The force field we used for the aMD

https://doi.org/10.1021/acsomega.4c06868
ACS Omega 2024, 9, 49422−49431

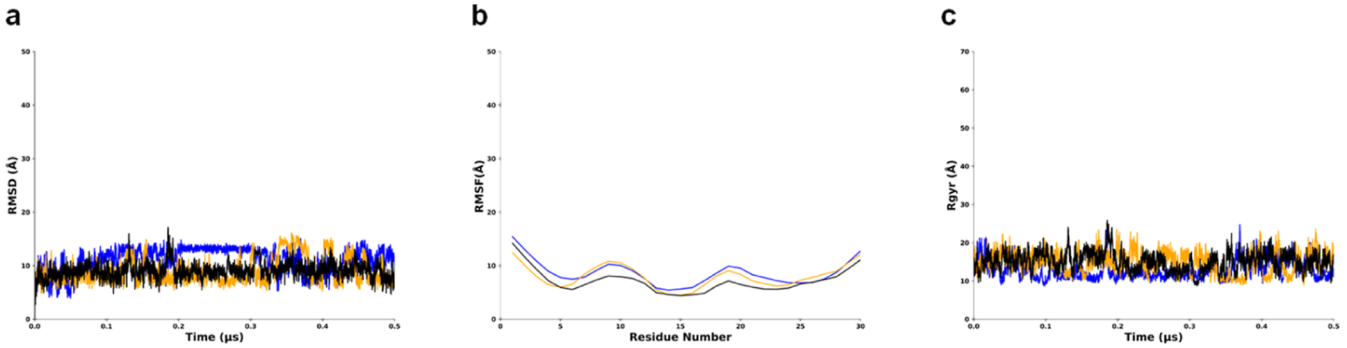

Figure 2. Behavior of N-terminal regions of LMP1 in MD simulations showing values around 25 Å or lesser for all the three graphs. Replicate 1 is in blue, replicate 2 is in orange, replicate 3 is in black. (a) RMSD graph. (b) RMSF graph. (c) Radius of gyration (Rg) plot.

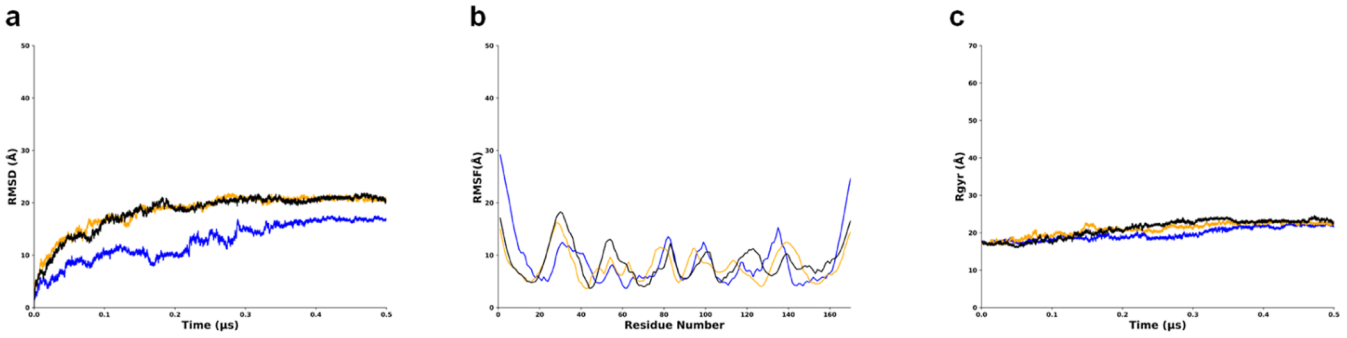

Figure 3. Behavior of TMD of LMP1 in MD simulations showing replicate 1 RMSD has a lower threshold compared to replicates 2 and 3. Replicate 1 is in blue, replicate 2 is in orange, and replicate 3 is in black. (a) RMSD graph. (b) RMSF graph. (c) Radius of gyration (Rg) plot.

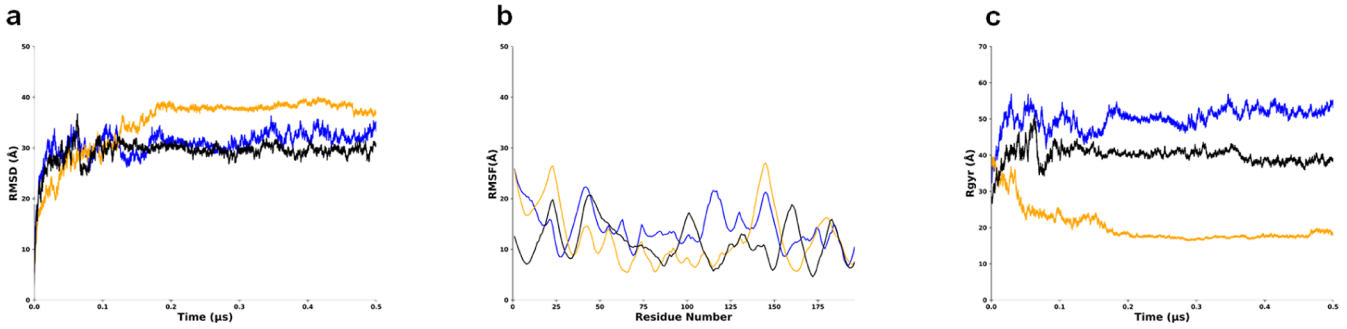

Figure 4. Behavior of C-terminal region of LMP1 in MD simulations with replicate 2 (RMSD and Rg) has a higher threshold from replicates 1 and 3. Replicate 1 is in blue, replicate 2 is in orange, and replicate 3 is in black. (a) RMSD graph. (b) RMSF graph. (c) Radius of gyration (Rg) plot.

simulation was the ff99SBdisp/tip4pd force field, originally developed for folded and disordered protein by Robustelli et al.[26] There was a recent study discussing the use of ff19SB/OPC force field for disordered protein aMD simulation; however, the study suggested the force field for the intrinsically disordered protein of less than 50 amino acids.[27] In our study, our LMP1 protein structure is more than 50 amino acids; hence, we used the ff99SBdisp/tip4pd field.

The aMD simulation revealed several noteworthy observations among the LMP1 protein domains or regions. The NTER domain showed root mean squared deviation (RMSD), and radius of gyration (Rg) reached a plateau at around the values of 10 Å indicating a stable structure (Figure 2a–c). NTER experiences structural fluctuations at residues Pro10 and Pro20 causing spikes in the root mean square fluctuation (RMSF) graph (Figure 2b). The consistent radius of gyration (Rg) value exhibits stability and folded structure of the protein (Figure 2c). The NTER domain's location may experience these fluctuations, suggesting functional flexibility, such as protein–ligand binding interfaces.

We noted that the TMD from replicate 1 has a lower threshold from replicates 2 and 3 which have similar values in RMSD, RMSF, and Rg. The TMD reached a plateau with an average RMSD value of 15 Å and remains low and steady throughout the simulation, indicating convergence to a structure (Figure 3a). The TMD RMSF is 15 Å with multiple fluctuations at residue Gly30, Phe50, Leu80, Leu120, and Leu140, indicating structural variations or flexibility in certain areas, such as flexible loops, protein termini, or solvent-exposed areas (Figure 3b). The Rg value is around 6 Å and is consistent throughout, indicating a more folded protein (Figure 3c).

In the meantime, for CTAR, RMSD value rises up to 30 Å indicating structural changes, but the simulation converges to a stable state (Figure 4). The RMSF value of 15 Å also suggests that the CTAR regions experience significant structural flexibility. The Rg values for CTAR varied but were around

https://doi.org/10.1021/acsomega.4c06868
ACS Omega 2024, 9, 49422–49431

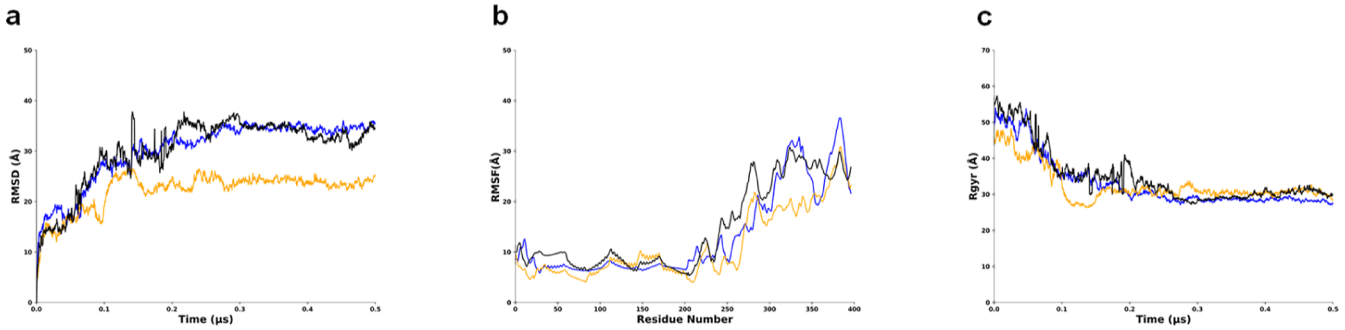

Figure 5. Behavior of LMP1 bilayer in MD simulations, showing replicate 2 (RMSD) has a lower threshold from the other two replicates. Replicate 1 is in blue, replicate 2 is in orange, and replicate 3 is in black. (a) RMSD graph. (b) RMSF graph. (c) Radius of gyration (Rg) plot.

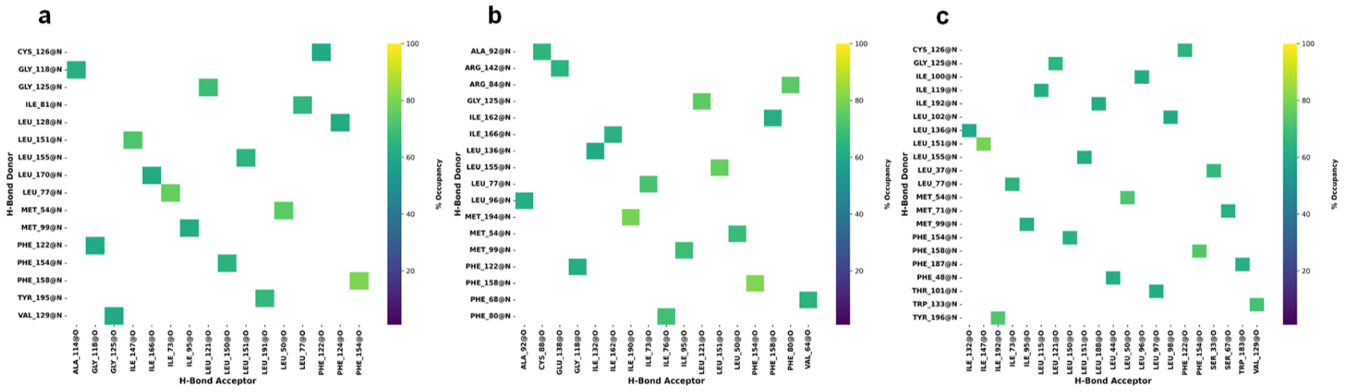

Figure 6. Intramolecular hydrogen bonding analysis for LMP1 bilayer triplicate data runs with a cutoff limit of 60%. (a) Replicate 1. (b) Replicate 2. (c) Replicate 3.

20 Å, and one of the triplicate runs (replicate 2) showed a downward graph trend, suggesting that the protein is becoming more compact or structurally constrained, or the simulation has converged (Figure 4c). The CTAR regions experience structural flexibility, possibly indicating functionally significant regions like protein−ligand binding interfaces or enzyme-active sites.

Meanwhile, the MD simulation revealed that the RMSD analysis in all the three replicates experiences fluctuation between 0.1 and 0.3 μs, indicating structural deviations and suggesting reduced flexibility in the LMP1 bilayer protein (Figure 5a). Interestingly, the Rg for LMP1 protein became more compact and stable as time passed, ranging from 35 to 45 Å for all three data (Figure 5c). RMSF analysis allowed us to identify that the increased flexibility in the LMP1 protein was mainly associated with the CTAR region (Figure 5b). One of the regions involves the residues from Gly300 until residue Asp396, whose average RMSF values were about 30 Å for all three data obtained. The RMSF value confirmed the flexibility structure in the CTAR regions, as stated by previous studies.[28,29] The studies by Izumi et al. and Mainou et al. emphasize not only the complex relationship of CTAR regions in B-lymphocyte growth transformation but also its unique role in mediating various signaling pathways such as NF-kB and c-Jun N-terminal kinase (JNK) pathways.

The presence of intrinsically disordered regions contributes to the flexibility and adaptability of LMP1, allowing it to interact with diverse binding partners and to exert its varied functions. Overall, LMP1 would not be classified as a purely intrinsically disordered protein. It contains structured domains alongside regions exhibiting intrinsic disorder, contributing to its unique functional properties.[15] Considering that some specific functions of intrinsically disordered regions within LMP1 are still under investigation, the intrinsic disorder of LMP1 can be affected by factors such as PTMs or binding interactions. Recent studies utilizing the proximity-dependent biotin identification method have revealed a complex interactome associated with LMP1, identifying over 1200 proteins that interact with LMP1 in various capacities, including direct, transient, or proximal associations.[30] Among these proteins, several are known to interact with the disordered regions of LMP1, particularly, the C-terminal activating regions (CTARs). For instance, TRAF proteins (TRAF1, TRAF2, TRAF3, TRAF5, and TRAF6) are crucial for LMP1 signaling and are known to bind to specific CTARs, facilitating the activation of downstream signaling pathways such as NF-κB and JNK.[31] The interactions of LMP1 with these TRAF proteins are particularly significant as they help to mediate the oncogenic effects of LMP1 in B-lymphocytes.[32]

2.3. Intramolecular Hydrogen Bonding Analysis.

Intramolecular hydrogen bonding is essential in stabilizing both the secondary and tertiary structure of proteins, contributing significantly to their overall conformational stability and native state.[33] The hydrogen bonding pattern is a key determinant of the final 3D structure adopted by the polypeptide chain. In this study, the LMP1 predicted structure was simulated for 0.5 μs, and we used the cutoff value of more than 60% for all the simulation runs (Figure 6).

Our analysis identified some fundamental interactions to explain the minimum ensembles of conformations. Six stable hydrogen bonding interactions, namely, between Phe154 and Phe158, Ile73 and Leu77, Leu50 and Met54, Leu121 and

https://doi.org/10.1021/acsomega.4c06868
ACS Omega 2024, 9, 49422−49431

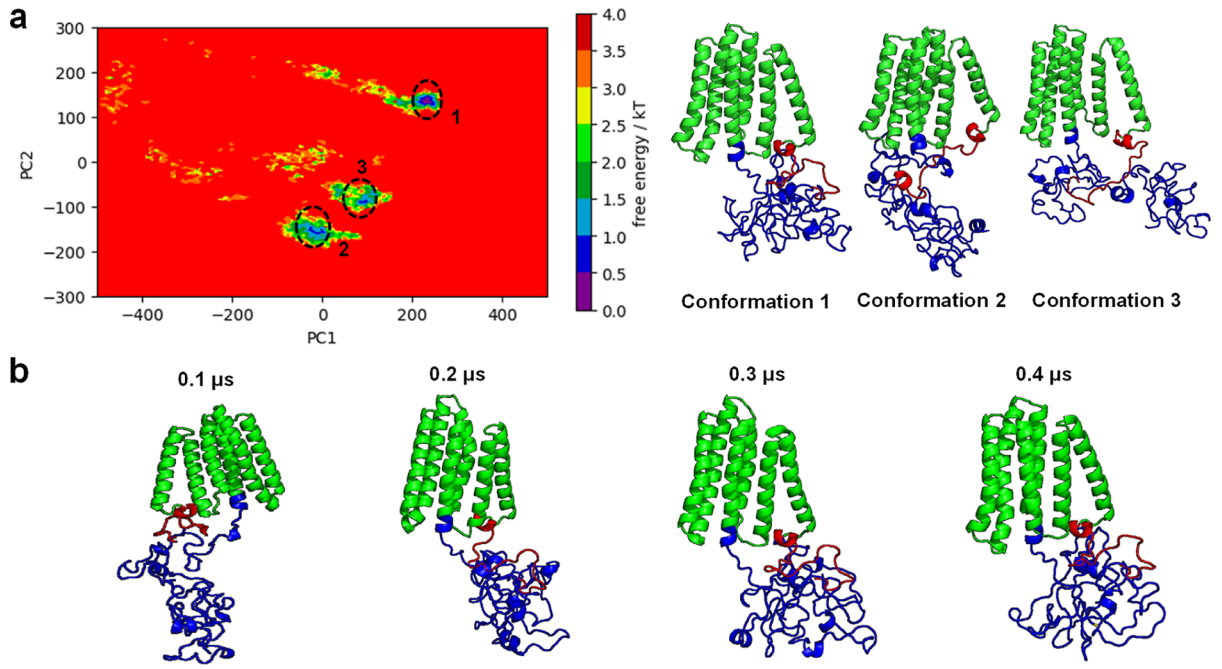

Figure 7. Combined FEL plot with the corresponding conformations of the three basins and the time evolution of LMP1 from replicate 1 that showed the steepest basin. (a) Combined FEL plot showed 3 basins which are conformation 1 (replicate 1), conformation 2 (replicate 2), and conformation 3 (replicate 3). (b) Time evolution of LMP1 from replicate 1 that showed the steepest free-energy basin. The TMD, NTER, and CTAR domains are shown in green, red, and blue, respectively.

Gly125, Leu151 and Leu155, and Ile95 with Met99 were found in all the triplicates run. Looking into the residue number position for all of these interactions, we can deduce that all of the stable hydrogen bonding interactions occur in the hydrophobic TMD of LMP1 (between amino acids 25 and 187). To date, there is no direct information available regarding hydrogen bonding in the TMD of LMP1. Hence, further experimental investigation needs to be conducted to provide insights into the presence, strength, and spatial arrangement of TMD intramolecular hydrogen bonding. TMD comprises approximately 160 amino acid residues that traverse the membrane and contribute to oligomerization and signal transmission (Supporting Information Figure S2a). TMD possesses the innate ability to form homo-oligomers, which may be detected as LMP1 patches in the membrane with the TMD5 playing a particularly important role in the oligomerization and activation of LMP1.[34,35] Recent research has demonstrated that an intermolecular interaction between TM3−6 and an FWLY motif in TMD1 promotes oligomerization and NF-kB signaling.[36] In addition, TMD forms a stable hairpin structure that anchors the protein to the membrane.[37]

2.4. Principle Component Analysis and Free-Energy Landscape. We used principal component analysis (PCA) and free-energy landscape (FEL) to analyze our LMP1 protein further as both analyses offer a comprehensive view of protein structure, dynamics, and stability. PCA identifies the key structural changes, and FEL provides the energetic driving forces behind these changes. The Supporting Information Figure S3 graph displays that the combined data for all of our simulation replicates suggested that there was less variance among all the replicate as the points converged toward the end of the time frame. This indicates that they are all similar in terms of the underlying features used in the PCA. Based on the PCA, the FEL plots were projected to identify the preferable conformations of the LMP1 protein (Figure 7a). The combined landscape appears to have three visible energy basins. These plots represent the relatively stable states of the protein. A ridge in the middle separates the two groups of plots, suggesting a transition state or barrier the protein must overcome to switch between the two stable states. The blue regions of the free energy indicate a more stable region; meanwhile, the yellow areas depict less stable areas.

Our PCA and FEL highlighted the analysis obtained from the RMSD and RMSF, whereby the plot showed the stable and less stable regions depicted by blue and yellow, respectively. The structure of LMP1 is highly dynamic, and it can undergo conformational changes that regulate its activity. Meanwhile, the RMSD and Rg values implied that the LMP1 bilayer protein structure has a reduced flexibility and compact structure. We observed that NTER remains stable throughout all the simulation runs; meanwhile, the CTAR region folded nearer to the TMD at the end of the simulation (Figure 7b).

Studies have revealed that LMP1 is a highly flexible protein that can adopt different conformations, depending on its binding partners and the cellular environment. The stability of NTER of LMP1 (Figure 7b) is essential for protein degradation via the ubiquitin-proteasome signaling pathway and cytoskeletal machinery interaction.[38,39] The NTER of LMP1 affects its half-life and the membrane insertion. If deleted, LMP1's activity and cytoskeleton connection are abolished, and a positive net charge is needed for correct membrane insertion.[40,41] A potential SH3-binding domain is also found between residues 9 and 20, whereby mutations in this location alter LMP1 patching and reduce EBV's ability to transform human primary B cells.[42] However, no protein-binding partners have been identified in LMP1's NTER domain.

Meanwhile, the conclusion of our MD simulation showed a crumpled CTAR domain structure (Figure 7b). CTAR1 domain consists of amino acids 194−232, whereas CTAR2 is

https://doi.org/10.1021/acsomega.4c06868
ACS Omega 2024, 9, 49422−49431

placed between amino acids 351 and 386. The lesser-known CTAR3 domain (amino acids 275−330) is also located between CTAR1 and CTAR2, with a few known interaction partners.[43] The CTAR of LMP1 contains multiple functional motifs that are involved in signal transduction. These motifs allow LMP1 to activate various signaling pathways, including the NF-κB pathway, the JAK/STAT pathway, and the MAPK pathway.[44−46] The CTAR domain (amino acids 187−386) attracts TRAFs and TRADD via PQQAT and PVQLSY sites, activating host cell signaling pathways.[47,48] The chains turn and coil at these PQQAT and PVQLSY sites, as demonstrated by our LMP1 protein molecular simulation (Supporting Information Figure S2b). It was also found that CTAR1 shares similarities with the CD40s PxQxT motif, which interacts with TRAF1−3 via the PVQET sequence.[49] Meanwhile, point mutations in LMP1's extreme carboxy terminus identified the core motif for CTAR2-mediated NF-kB activation.[50]

3. CONCLUSIONS

This work continued our previous work and presented an informational structure on EBV LMP1 using an aMD simulation. We have employed other protein structure websites, such as AlphaFold2 and GalaxyWeb, to confirm our structure better. With little to no known full-length structure of LMP1, our study can be a stepping stone for more research, particularly in the cancer drug discovery field. With convenient and user-friendly web tools such as CHARMM-graphical user interface (GUI), we were able to generate the 1-palmitoyl-2-oleoyl-phosphatidylcholine (POPC) lipid bilayer membrane for LMP1 for MD simulation. The protein simulation produced a free-energy landscape that displayed conformational diversity, particularly in the CTAR region. It revealed that our LMP1 protein structure has a compact structure and reduced flexibility. Despite the diversity, the generated LMP1 conformational ensemble produced states that showed compacted folds, as in the TMD region. Our hydrogen bonding analysis also identified some exciting interactions to explain the minimum ensembles of conformations. Although there were some differences in the hydrogen bonding results among our triplicate runs, we have addressed the possible reasons for these discrepancies. The structure of LMP1 is highly dynamic, and it can undergo conformational changes that regulate its activity. Understanding the entire structure of LMP1 is essential for developing new therapies for EBV-associated malignancies. By targeting specific domains or functional motifs of LMP1, it may be possible to create drugs that inhibit its oncogenic activity. This study demonstrates that with further experimental validation of the structure−function relationship, our predicted full-length LMP1 protein structure has the potential to be used for future drug discovery studies.

4. COMPUTATIONAL METHODS

4.1. System Setting and Modeling. The complete LMP1 sequences (386 amino acids) were retrieved from UniProt.[51] The LMP1 protein used here was designed based on our previous study.[16]

4.2. Protein Structure Prediction Website. Some widely used protein structure prediction tools, such as GalaxyWeb and AlphaFold2, were used to reconfirm the LMP1 predicted protein structure we designed. GalaxyWeb has a web server specifically designed to predict the structure of protein homo-oligomers called Galaxy Homomer. These are proteins that are formed by the assembly of identical subunits. It uses two approaches, namely, template-based modeling and ab initio docking. In our LMP1 predicted structure, the Galaxy Homomer uses the ab initio technique.[52] Meanwhile, Alphafold2 generated 10 PDB files based on credibility ratings to assess the anticipated model's quality. One was the pLDDT score, which measures the accuracy of the prediction. The pLDDT is a key metric used by AlphaFold2 to assess the confidence of its protein structure predictions. The pLDDT scores range from 0 to 100, where higher values indicate greater confidence in the accuracy of the predicted residue structure. pLDDT values above 90 suggest incredibly high precision in the predicted structure. Values between 70 and 90 suggest good accuracy and moderate confidence. Meanwhile, values ranging less than 70 reflect poorer accuracy or less reliable predictions.

4.3. Lipid Membrane Modeling. The initial lipid membrane structures were built using the CHARMM-GUI membrane builder.[53] It is a web-based GUI for generating input files for the LMP1 lipid bilayer. POPC is the lipid bilayer membrane. It is a zwitterionic molecule and a neutral phospholipid commonly used in MDs simulations to model biological membranes because it is a significant component of cell membranes and forms stable bilayers.[54] POPC lipids are the predominant lipids found in the organelles of mammalian cells, such as the plasma membrane, endoplasmic reticulum, and Golgi apparatus.[55] This abundance enables a highly accurate representation of the local environment of the peptides within the lipid bilayer, especially when the system is surrounded by an adequate number of water molecules.[56] The CHARMM-GUI membrane-generated output files in the parm7 and rst7 formats were then used for the protein simulation in AMBER. In the current study, our scope was specifically focused on modeling and simulating the full LMP1 protein structure without palmitoylation modifications. While we acknowledge that palmitoylation at Cys78 plays a significant role in LMP1's localization,[57] previous studies have demonstrated that LMP1 maintains its ability to associate with lipid rafts even when palmitoylation is disrupted, though potentially with modified efficiency.[58] This suggests the existence of additional mechanisms contributing to LMP1's localization and function beyond palmitoylation. In the future, we would investigate the conformational landscapes of both palmitoylated and nonpalmitoylated LMP1, specifically focusing on how these states influence lipid raft associations. This work will provide valuable insights into the structural dynamics of LMP1.

4.4. Molecular Dynamic Simulations. aMD is a simulation technique designed to enhance conformational sampling by modifying the potential energy landscape.[59] This method allows for the exploration of conformations that are typically less accessible due to high energy barriers, thus facilitating the observation of native-like structures and mitigating the sampling of spurious conformations during molecular simulations. In addition, the aMD helps maintain residue proximity to the membrane, which is crucial for studying membrane proteins or proteins with membrane-associated domains. One of the first steps necessary to simulate aMD is to do a classical molecular dynamic simulation to obtain the average total potential energy threshold (EthreshP) and average dihedral angle energy threshold (EthreshD) as these parameters are needed as input for the aMD simulation. LMP1 EthreshP and EthreshD triplicate run averages were

https://doi.org/10.1021/acsomega.4c06868
ACS Omega 2024, 9, 49422−49431

−512163.333 kcal/mol and 6428 kcal/mol, respectively. The AMBER 20 MD package performed an adapted LMP1MD simulation based on AMBER's aMD tutorial.[60] For conventional MD simulation, the preparation stages of minimization, equilibration, and heating were carried out using ff99SB, lipid21, and TIP4PD force field. The particle mesh Ewald cutoff distance was kept at 10 Å, and the restraint force was held at 300 kcal/mol. Subsequently, heating was carried out for 20 ps, gradually increasing the temperature from 0 to 300 K along the *NVT* ensemble. During the equilibration stage with a time step of 500 ps, we employed the *NPT* ensemble followed by the preparatory production stage for 5 ns. Additional parameters were calculated for aMD simulation: EthreshP, average total potential energy threshold; alphaP, inverse strength boost factor for the total potential energy; EthreshD, average dihedral energy threshold; and alphaD, inverse strength boost factor for the dihedral energy. The aMD production stage was carried out for 0.5 μs and in triplicates (replicates 1, 2, and 3).

4.5. Analysis. Analyses were performed using CPPTRAJ on AMBER 20 for trajectory analysis, while visual molecular dynamics and PyMOL were used to visualize and check the MDs simulations in real-time and postprocessing.[61−63] PCA was performed by calculating the covariance matrix and diagonalizing it to identify the principal components (PCs) and their corresponding eigenvalues. The top PCs represent the most significant variations in the protein motion. We estimate the free energy from PCA by projecting the protein coordinates from each trajectory frame onto the top few PCs (usually PROJ1 and PROJ2). This reduces the dimensionality of the data for analysis. Boltzmann distribution is used to estimate the free energy

$$G(i) = -kT \times \ln(N(i)/N_{max})$$

where:

$G(i)$ is the free energy at point i in the PC space. k is Boltzmann's constant. T is the absolute temperature of the simulation. $N(i)$ is the probability density of finding the protein at point i. N_{max} is the maximum probability density in the data set.

FEL was visualized by constructing a 2D contour plot using axes of the first two principal components (PROJ1 vs PROJ2). Regions with lower free-energy values correspond to more populated and stable protein conformations, while higher values indicate less probable and potentially transition states.

■ ASSOCIATED CONTENT

Data Availability Statement

All MD simulations were performed using Assisted Model Building with Energy Refinement (AMBER; version 20), utilizing a free academic license from the Swinburne Supercomputing OzSTAR Facility. The input files for the MD simulations, which include topologies and parameters, are available in the Zenodo Database via the provided link: https://zenodo.org/records/14189529.

Supporting Information

The Supporting Information is available free of charge at https://pubs.acs.org/doi/10.1021/acsomega.4c06868.

Ab initio docking results for LMP1 predicted structure; per-residue confidence score for LMP1 model 3; AlphaFold2 LMP1 model 3 image; molecular image of TMD and N-terminal domain of the LMP1 protein; CTAR1 and CTAR2 domains; and combined PCA data for all the triplicate runs (PDF)

■ AUTHOR INFORMATION

Corresponding Authors

Xavier Chee Wezen − *Faculty of Engineering, Computing and Science, Swinburne University of Technology Sarawak, Kuching 93350, Malaysia; Department of Biochemistry, Yong Loo Lin School of Medicine, National University of Singapore, Singapore 117596, Singapore;* orcid.org/0000-0001-8497-5953; Email: xchee@swinburne.edu.my

Taufiq Rahman − *Department of Pharmacology, University of Cambridge, Cambridge CB2 1PD, U.K.;* orcid.org/0000-0003-3830-5160; Email: mtur2@cam.ac.uk

Authors

Dayang-Sharyati D. A. Salam − *Faculty of Engineering, Computing and Science, Swinburne University of Technology Sarawak, Kuching 93350, Malaysia*

Kavinda Kashi Juliyan Gunasinghe − *Faculty of Engineering, Computing and Science, Swinburne University of Technology Sarawak, Kuching 93350, Malaysia;* orcid.org/0000-0003-0242-0271

Siaw San Hwang − *Faculty of Engineering, Computing and Science, Swinburne University of Technology Sarawak, Kuching 93350, Malaysia*

Irine Runnie Henry Ginjom − *Faculty of Engineering, Computing and Science, Swinburne University of Technology Sarawak, Kuching 93350, Malaysia*

Complete contact information is available at: https://pubs.acs.org/10.1021/acsomega.4c06868

Author Contributions

D.-S.D.A.S.: conception and design of the work; analysis and interpretation of data; and drafted the work. K.K.J.G.: interpretation of data, revised, and editing. S.S.H.: revised and editing. I.R.H.G.: revised and editing. T.R.: revised and editing. X.C.W.: interpretation of data, revised, and editing.

Notes

The authors declare no competing financial interest.

■ REFERENCES

(1) de-Thé, G.; Day, N. E.; Geser, A.; Lavoué, M. F.; Ho, J. H.; Simons, M. J.; Sohier, R.; Tukei, P.; Vonka, V.; Zavadova, H. Sero-epidemiology of the Epstein-Barr virus: preliminary analysis of an international study − a review. *IARC Sci. Publ.* **1975**, No. 11 Pt 2, 3−16.

(2) Pratt, Z. L.; Zhang, J.; Sugden, B. The Latent Membrane Protein 1 (LMP1) Oncogene of Epstein-Barr Virus Can Simultaneously Induce and Inhibit Apoptosis in B Cells. *J. Virol.* **2012**, *86* (8), 4380−4393.

(3) Patel, P. D.; Alghareeb, R.; Hussain, A.; Maheshwari, M. V.; Khalid, N. The Association of Epstein-Barr Virus With Cancer. *Cureus* **2022**, *14* (6), No. e26314.

(4) Kaye, K. M.; Izumi, K. M.; Kieff, E. Epstein-Barr virus latent membrane protein 1 is essential for B-lymphocyte growth transformation. *Proc. Natl. Acad. Sci. U.S.A.* **1993**, *90* (19), 9150−9154.

(5) Eliopoulos, A. G.; Blake, S. M.; Floettmann, J. E.; Rowe, M.; Young, L. S. Epstein-Barr virus-encoded latent membrane protein 1 activates the JNK pathway through its extreme C terminus via a mechanism involving TRADD and TRAF2. *J. Virol.* **1999**, *73* (2), 1023−1035.

(6) Uchida, J.; Yasui, T.; Takaoka-Shichijo, Y.; Muraoka, M.; Kulwichit, W.; Raab-Traub, N.; Kikutani, H. Mimicry of CD40 signals

by Epstein-Barr virus LMP1 in B lymphocyte responses. *Science* **1999**, *286* (5438), 300−303.
(7) Kieser, A.; Kaiser, C.; Hammerschmidt, W. LMP1 signal transduction differs substantially from TNF receptor 1 signaling in the molecular functions of TRADD and TRAF2. *EMBO J.* **1999**, *18* (9), 2511−2521.
(8) Rastelli, J.; Hömig-Hölzel, C.; Seagal, J.; Müller, W.; Hermann, A. C.; Rajewsky, K.; Zimber-Strobl, U. LMP1 signaling can replace CD40 signaling in B cells in vivo and has unique features of inducing class-switch recombination to IgG1. *Blood* **2008**, *111* (3), 1448−1455.
(9) Ersing, I.; Bernhardt, K.; Gewurz, B. E. NF-κB and IRF7 Pathway Activation by Epstein-Barr Virus Latent Membrane Protein 1. *Viruses* **2013**, *5* (6), 1587−1606.
(10) Dawson, C. W.; Port, R. J.; Young, L. S. The role of the EBV-encoded latent membrane proteins LMP1 and LMP2 in the pathogenesis of nasopharyngeal carcinoma (NPC). *Semin. Cancer Biol.* **2012**, *22* (2), 144−153.
(11) Cameron, J. E.; Yin, Q.; Fewell, C.; Lacey, M.; McBride, J.; Wang, X.; Lin, Z.; Schaefer, B. C.; Flemington, E. K. Epstein-Barr virus latent membrane protein 1 induces cellular MicroRNA miR-146a, a modulator of lymphocyte signaling pathways. *J. Virol.* **2008**, *82* (4), 1946−1958.
(12) Eliopoulos, A. G.; Young, L. S. LMP1 structure and signal transduction. *Semin. Cancer Biol.* **2001**, *11* (6), 435−444.
(13) Gires, O.; Zimber-Strobl, U.; Gonnella, R.; Ueffing, M.; Marschall, G.; Zeidler, R.; Pich, D.; Hammerschmidt, W. Latent membrane protein 1 of Epstein−Barr virus mimics a constitutively active receptor molecule. *EMBO J.* **1997**, *16*, 6131−6140.
(14) Mainou, B. A.; Everly, D. N.; Raab-Traub, N. Unique signaling properties of CTAR1 in LMP1-mediated transformation. *J. Virol.* **2007**, *81* (18), 9680−9692.
(15) Kieser, A.; Sterz, K. R. The latent membrane protein 1 (LMP1). *Curr. Top. Microbiol. Immunol.* **2015**, *391*, 119−149.
(16) Salam, D. S. D.; San Hwang, S.; Wang, F.; Lau, B. T.; Chee, X. W. In silico strategy to model LMP1 of Epstein−Barr virus protein. In *2023 IEEE International Conference on Bioinformatics and Biomedicine (BIBM)*; IEEE, 2023, pp 2741−2747.
(17) Kjaergaard, M.; Kragelund, B. B. Functions of intrinsic disorder in transmembrane proteins. *Cell. Mol. Life Sci.* **2017**, *74*, 3205−3224.
(18) Jumper, J.; Evans, R.; Pritzel, A.; Green, T.; Figurnov, M.; Ronneberger, O.; Tunyasuvunakool, K.; Bates, R.; Žídek, A.; Potapenko, A.; Bridgland, A.; et al. Highly accurate protein structure prediction with AlphaFold. *Nature* **2021**, *596* (7873), 583−589.
(19) Keskin Karakoyun, H.; Yüksel, Ş. K.; Amanoglu, I.; Naserikhojasteh, L.; Yeşilyurt, A.; Yakıcıer, C.; Timuçin, E.; Akyerli, C. B. Evaluation of AlphaFold structure-based protein stability prediction on missense variations in cancer. *Front. Genet.* **2023**, *14*, 1052383.
(20) Weng, Y.; Pan, C.; Shen, Z.; Chen, S.; Xu, L.; Dong, X.; Chen, J. Identification of potential WSB1 inhibitors by AlphaFold Modeling, virtual screening, and molecular dynamics simulation studies. *J. Evidence-Based Complementary Altern. Med.* **2022**, *2022* (1), 4629392.
(21) Goulet, A.; Cambillau, C.; Roussel, A.; Imbert, I. Structure prediction and analysis of hepatitis E virus non-structural proteins from the replication and transcription machinery by AlphaFold2. *Viruses* **2022**, *14* (7), 1537.
(22) Mani, H.; Chang, C. C.; Hsu, H. J.; Yang, C. H.; Yen, J. H.; Liou, J. W. Comparison, Analysis, and Molecular Dynamics Simulations of Structures of a Viral Protein Modeled Using Various Computational Tools. *Bioengineering* **2023**, *10* (9), 1004.
(23) Veit, M.; Gadalla, M. R.; Zhang, M. Using Alphafold2 to Predict the Structure of the Gp5/M Dimer of Porcine Respiratory and Reproductive Syndrome Virus. *Int. J. Mol. Sci.* **2022**, *23* (21), 13209.
(24) Gires, O.; Zimber-Strobl, U.; Gonnella, R.; Ueffing, M.; Marschall, G.; Zeidler, R.; Pich, D.; Hammerschmidt, W. Latent membrane protein 1 of Epstein-Barr virus mimics a constitutively active receptor molecule. *EMBO J.* **1997**, *16* (20), 6131−6140.
(25) Wrobel, C. M.; Geiger, T. R.; Nix, R. N.; Robitaille, A. M.; Weigand, S.; Cervantes, A.; Gonzalez, M.; Martin, J. M. High molecular weight complex analysis of Epstein-Barr virus Latent Membrane Protein 1 (LMP-1): structural insights into LMP-1's homo-oligomerization and lipid raft association. *Virus Res.* **2013**, *178* (2), 314−327.
(26) Robustelli, P.; Piana, S.; Shaw, D. E. Developing a molecular dynamics force field for both folded and disordered protein states. *Proc. Natl. Acad. Sci. U.S.A.* **2018**, *115* (21), E4758−E4766.
(27) Coppa, C.; Bazzoli, A.; Barkhordari, M.; Contini, A. Accelerated Molecular Dynamics for Peptide Folding: Benchmarking Different Combinations of Force Fields and Explicit Solvent Models. *J. Chem. Inf. Model.* **2023**, *63* (10), 3030−3042.
(28) Izumi, K. M.; McFarland, E. D. C.; Riley, E. A.; Rizzo, D.; Chen, Y.; Kieff, E. The residues between the two transformation effector sites of Epstein-Barr virus latent membrane protein 1 are not critical for B-lymphocyte growth transformation. *J. Virol.* **1999**, *73* (12), 9908−9916.
(29) Mainou, B. A.; Everly, D. N.; Raab-Traub, N. Unique signaling properties of CTAR1 in LMP1-mediated transformation. *J. Virol.* **2007**, *81* (18), 9680−9692.
(30) Nkosi, D.; Sun, L.; Duke, L. C.; Patel, N.; Surapaneni, S. K.; Singh, M.; Meckes, D. G. Epstein-barr virus lmp1 promotes syntenin-1- and hrs-induced extracellular vesicle formation for its own secretion to increase cell proliferation and migration. *Mbio* **2020**, *11* (3), No. e00589.
(31) Rider, M. A.; Cheerathodi, M. R.; Hurwitz, S. N.; Nkosi, D.; Howell, L. A.; Tremblay, D. C.; Liu, X.; Zhu, F.; Meckes, D. G., Jr. The interactome of EBV LMP1 evaluated by proximity-based bioid approach. *Virology* **2018**, *516*, 55−70.
(32) Graham, J.; Arcipowski, K.; Bishop, G. Differential b-lymphocyte regulation by cd40 and its viral mimic, latent membrane protein 1. *Immunol. Rev.* **2010**, *237* (1), 226−248.
(33) Pace, C. N.; Fu, H.; Lee Fryar, K.; Landua, J.; Trevino, S. R.; Schell, D.; Thurlkill, R. L.; Imura, S.; Scholtz, J. M.; Gajiwala, K.; Sevcik, J.; Urbanikova, L.; Myers, J. K.; Takano, K.; Hebert, E. J.; Shirley, B. A.; Grimsley, G. R. Contribution of hydrogen bonds to protein stability. *Protein Sci.* **2014**, *23* (5), 652−661.
(34) Liebowitz, D.; Wang, D.; Kieff, E. Orientation and patching of the latent infection membrane protein encoded by Epstein-Barr virus. *J. Virol.* **1986**, *58*, 233−237.
(35) Wang, X.; Fiorini, Z.; Smith, C.; Zhang, Y.; Li, J.; Watkins, L. R.; Yin, H. Repositioning antimicrobial agent pentamidine as a disruptor of the lateral interactions of transmembrane domain 5 of EBV latent membrane protein 1. *PLoS One* **2012**, *7* (10), No. e47703.
(36) Soni, V.; Yasui, T.; Cahir-McFarland, E.; Kieff, E. LMP1 Transmembrane Domain 1 and 2 (TM1-2) FWLY Mediates Intermolecular Interactions with TM3-6 To Activate NF-κB. *J. Virol.* **2006**, *80* (21), 10787−10793.
(37) Lee, J.; Sugden, B. A membrane leucine heptad contributes to trafficking, signaling, and transformation by latent membrane protein 1. *J. Virol.* **2007**, *81* (17), 9121−9130.
(38) Martin, J.; Sugden, B. Transformation by the oncogenic latent membrane protein correlates with its rapid turnover, membrane localization, and cytoskeletal association. *J. Virol.* **1991**, *65* (6), 3246−3258.
(39) Aviel, S.; Winberg, G.; Massucci, M.; Ciechanover, A. Degradation of the Epstein-Barr virus latent membrane protein 1 (LMP1) by the ubiquitin-proteasome pathway: targeting via ubiquitination of the N-terminal residue. *J. Biol. Chem.* **2000**, *275* (31), 23491−23499.
(40) Wang, D.; Liebowitz, D.; Wang, F.; Gregory, C.; Rickinson, A.; Larson, R.; Springer, T.; Kieff, E. Epstein-Barr virus latent infection membrane protein alters the human B-lymphocyte phenotype: deletion of the amino terminus abolishes activity. *J. Virol.* **1988**, *62*, 4173−4184.
(41) Coffin, W. F.; Erickson, K. D.; Hoedt-Miller, M.; Martin, J. M. The cytoplasmic amino-terminus of the Latent Membrane Protein-1 of Epstein-Barr Virus: relationship between transmembrane orienta-

https://doi.org/10.1021/acsomega.4c06868
ACS Omega 2024, 9, 49422−49431

tion and effector functions of the carboxy-terminus and transmembrane domain. *Oncogene* **2001**, *20*, 5313−5330.
(42) Bloss, T.; Kaykas, A.; Sugden, B. Dissociation of patching by latent membrane protein-1 of Epstein−Barr virus from its stimulation of NF-κB activity. *J. Gen. Virol.* **1999**, *80*, 3227−3232.
(43) Fielding, C. A.; Sandvej, K.; Mehl, A.; Brennan, P.; Jones, M.; Rowe, M. Epstein-Barr virus LMP-1 natural sequence variants differ in their potential to activate cellular signaling pathways. *J. Virol.* **2001**, *75* (19), 9129−9141.
(44) Paine, E.; Scheinman, R. I.; Baldwin, A. S., Jr.; Raab-Traub, N. Expression of LMP1 in epithelial cells leads to the activation of a select subset of NF-kappa B/Rel family proteins. *J. Virol.* **1995**, *69* (7), 4572−4576.
(45) Uemura, N.; Kajino, T.; Sanjo, H.; Sato, S.; Akira, S.; Matsumoto, K.; Ninomiya-Tsuji, J. TAK1 is a component of the Epstein-Barr virus LMP1 complex and is essential for activation of JNK but not of NF-κB. *J. Biol. Chem.* **2006**, *281* (12), 7863−7872.
(46) Wan, J.; Zhang, W.; Wu, L.; Bai, T.; Zhang, M.; Lo, K.-W.; Chui, Y.-L.; Cui, Y.; Tao, Q.; Yamamoto, M.; et al. BS69, a specific adaptor in the latent membrane protein 1-mediated c-Jun N-terminal kinase pathway. *Mol. Cell. Biol.* **2006**, *26* (2), 448−456.
(47) Miller, W. E.; Cheshire, J. L.; Raab-Traub, N. Interaction of tumor necrosis factor receptor-associated factor signaling proteins with the latent membrane protein 1 PXQXT motif is essential for induction of epidermal growth factor receptor expression. *Mol. Cell. Biol.* **1998**, *18* (5), 2835−2844.
(48) Schneider, F.; Neugebauer, J.; Griese, J.; Liefold, N.; Kutz, H.; Briseño, C.; Kieser, A. The viral oncoprotein LMP1 exploits TRADD for signaling by masking its apoptotic activity. *PLoS Biol.* **2008**, *6* (1), No. e8.
(49) Pullen, S. S.; Dang, T. T. A.; Crute, J. J.; Kehry, M. R. CD40 Signaling through Tumor Necrosis Factor Receptor-associated Factors (TRAFs). *J. Biol. Chem.* **1999**, *274*, 14246−14254.
(50) Floettmann, J. E.; Rowe, M. Epstein-Barr virus latent membrane protein-1 (LMP1) C-terminus activation region 2 (CTAR2) maps to the far C-terminus and requires oligomerisation for NF-κB activation. *Oncogene* **1997**, *15*, 1851−1858.
(51) The UniProt Consortium. UniProt: the Universal Protein Knowledgebase in 2023. *Nucleic Acids Res.* **2023**, *51* (D1), D523−D531.
(52) Ko, J.; Park, H.; Heo, L.; Seok, C. GalaxyWEB server for protein structure prediction and refinement. *Nucleic Acids Res.* **2012**, *40* (W1), W294−W297.
(53) Lee, J.; Patel, D. S.; Ståhle, J.; Park, S.-J.; Kern, N. R.; Kim, S.; Lee, J.; Cheng, X.; Valvano, M. A.; Holst, O.; Knirel, Y. A.; et al. CHARMM-GUI membrane builder for complex biological membrane simulations with glycolipids and lipoglycans. *J. Chem. Theory Comput.* **2018**, *15* (1), 775−786.
(54) Pasenkiewicz-Gierula, M.; Murzyn, K.; Róg, T.; Czaplewski, C. Molecular dynamics simulation studies of lipid bilayer systems. *Acta Biochim. Pol.* **2000**, *47* (3), 601−611.
(55) Van Meer, G.; de Kroon, A. I. P. M. Lipid map of the mammalian cell. *J. Cell Sci.* **2011**, *124* (1), 5−8.
(56) Wang, C. W.; Fischer, W. B. Rotational Dynamics of The Transmembrane Domains Play an Important Role in Peptide Dynamics of Viral Fusion and Ion Channel Forming Proteins-A Molecular Dynamics Simulation Study. *Viruses* **2022**, *14* (4), 699.
(57) Higuchi, M.; Izumi, K.; Kieff, E. Epstein−barr virus latent-infection membrane proteins are palmitoylated and raft-associated: protein 1 binds to the cytoskeleton through tnf receptor cytoplasmic factors. *Proc. Natl. Acad. Sci. U.S.A.* **2001**, *98* (8), 4675−4680.
(58) Katzman, R.; Longnecker, R. Lmp2a does not require palmitoylation to localize to buoyant complexes or for function. *J. Virol.* **2004**, *78* (20), 10878−10887.
(59) Hamelberg, D.; Mongan, J.; McCammon, J. A. Accelerated molecular dynamics: a promising and efficient simulation method for biomolecules. *J. Chem. Phys.* **2004**, *120* (24), 11919−11929.
(60) Case, D. A.; Aktulga, H. M.; Belfon, K.; Ben-Shalom, I. Y.; Berryman, J. T.; Brozell, S. R.; Cerutti, D. S.; Cheatham, T. E.; Cisneros, G. A.; Cruzeiro, V. W. D.; Darden, T. A.; Forouzesh, N.; Giambaşu, G.; Giese, T.; Gilson, M. K.; Gohlke, H.; Goetz, A. W.; Harris, J.; Izadi, S.; Izmailov, S. A.; Kasavajhala, K.; Kaymak, M. C.; King, E.; Kovalenko, A.; Kurtzman, T.; Lee, T. S.; Li, P.; Lin, C.; Liu, J.; Luchko, T.; Luo, R.; Machado, M.; Man, V.; Manathunga, M.; Merz, K. M.; Miao, Y.; Mikhailovskii, O.; Monard, G.; Nguyen, H.; O'Hearn, K. A.; Onufriev, A.; Pan, F.; Pantano, S.; Qi, R.; Rahnamoun, A.; Roe, D. R.; Roitberg, A.; Sagui, C.; Schott-Verdugo, S.; Shajan, A.; Shen, J.; Simmerling, C. L.; Skrynnikov, N. R.; Smith, J.; Swails, J.; Walker, R. C.; Wang, J.; Wang, J.; Wei, H.; Wu, X.; Wu, Y.; Xiong, Y.; Xue, Y.; York, D. M.; Zhao, S.; Zhu, Q.; Kollman, P. A. *Amber 2023*; University of California: San Francisco, 2023.
(61) Roe, D. R.; Cheatham, T. E., III PTRAJ and CPPTRAJ: Software for Processing and Analysis of Molecular Dynamics Trajectory Data. *J. Chem. Theory Comput.* **2013**, *9* (7), 3084−3095.
(62) Humphrey, W.; Dalke, A.; Schulten, K. VMD: visual molecular dynamics. *J. Mol. Graphics* **1996**, *14* (1), 33−38.
(63) Schrödinger, L.; DeLano, W. PyMOL, 2020. http://www.pymol.org/pymol.

https://doi.org/10.1021/acsomega.4c06868
ACS Omega 2024, 9, 49422−49431